Resolution of conductive-radiative heat transfer in a semi-transparent medium: functional estimation of the radiative source term with Monte Carlo method

Léa Penazzi, Olivier Farges, Yves Jannot, Johann Meulemans, Vincent Schick

▶ **To cite this version:**

Léa Penazzi, Olivier Farges, Yves Jannot, Johann Meulemans, Vincent Schick. Resolution of conductive-radiative heat transfer in a semi-transparent medium: functional estimation of the radiative source term with Monte Carlo method. International Heat Transfer Conference 17, Aug 2023, Cape Town, South Africa. pp.10, 10.1615/IHTC17.50-130 . hal-04362765v2

HAL Id: hal-04362765
https://hal.science/hal-04362765v2

Submitted on 16 Jan 2024

HAL is a multi-disciplinary open access archive for the deposit and dissemination of scientific research documents, whether they are published or not. The documents may come from teaching and research institutions in France or abroad, or from public or private research centers.

L'archive ouverte pluridisciplinaire **HAL**, est destinée au dépôt et à la diffusion de documents scientifiques de niveau recherche, publiés ou non, émanant des établissements d'enseignement et de recherche français ou étrangers, des laboratoires publics ou privés.

Resolution of conductive-radiative heat transfer in a semi-transparent medium: functional estimation of the radiative source term with Monte Carlo method

Léa Penazzi, Olivier Farges, Yves Jannot, Johann Meulemans, Vincent Schick

▶ **To cite this version:**

Léa Penazzi, Olivier Farges, Yves Jannot, Johann Meulemans, Vincent Schick. Resolution of conductive-radiative heat transfer in a semi-transparent medium: functional estimation of the radiative source term with Monte Carlo method. International Heat Transfer Conference 17, Aug 2023, Cape Town, France. pp.10, 10.1615/IHTC17.50-130 . hal-04362765

HAL Id: hal-04362765
https://hal.science/hal-04362765

Submitted on 23 Dec 2023

HAL is a multi-disciplinary open access archive for the deposit and dissemination of scientific research documents, whether they are published or not. The documents may come from teaching and research institutions in France or abroad, or from public or private research centers.

L'archive ouverte pluridisciplinaire **HAL**, est destinée au dépôt et à la diffusion de documents scientifiques de niveau recherche, publiés ou non, émanant des établissements d'enseignement et de recherche français ou étrangers, des laboratoires publics ou privés.

Proceedings of the 17th International Heat Transfer Conference, IHTC-17
14 - 18 August 2023, Cape Town, South Africa

IHTC-17 | ID: 1007

RESOLUTION OF CONDUCTIVE-RADIATIVE HEAT TRANSFER IN A SEMI-TRANSPARENT MEDIUM: FUNCTIONAL ESTIMATION OF THE RADIATIVE SOURCE TERM WITH MONTE CARLO METHOD

L. Penazzi [1,2*], O. Farges [1,2], Y. Jannot [1,2], J. Meulemans [2,3], V. Schick [1,2]

[1]Université de Lorraine, CNRS, LEMTA, F-54500 Vandoeuvre-lès-Nancy, France
[2]Laboratoire Commun Canopée, CNRS, Université de Lorraine, Saint-Gobain, France
[3]Saint-Gobain Research Paris, 39 quai Lucien Lefranc, F-93303 Aubervilliers, France

ABSTRACT

To estimate materials' thermo–physical properties at high temperatures, there is a need of robust direct models that can be solved quickly and account for the strong coupling between conduction and radiation. This study investigates using the Monte Carlo method to solve a conduction–radiation model in a semi–transparent material in a reduced computational time. Transient conduction in an absorbing/emitting and non-scattering grey medium in an academic configuration is investigated. The radiative source term of the heat equation is estimated as a function of the temperature field to the power 4, using a Finite Differences algorithm and a single Monte Carlo simulation to solve radiation. The numerical study shows that the results are in good agreement with the literature and that the functional estimation of the radiative source term allows coupled model resolution in less computing time that the standard approaches, such as Finite Volumes or Elements Methods. Indeed, the coefficients of the function were obtained in 4h with the Monte Carlo computation on an academic calculation server. 15 different configurations were then solved in less than 1min in transient state configurations and less than 6min at steady state configurations with the Finite Differences Method on a conventional laptop. This function is obtained without any compromise on the complexity of the coupled physics or the geometry. Because of the latter features, using this method in inversion processes becomes easible, as the direct model must be evaluated a large number of times.

KEYWORDS: Conduction, Radiation, Semi–transparent medium, Monte Carlo method, Transfer function

1. INTRODUCTION

To optimize the use of insulating materials in high temperature processes, developing measurements methods to characterize the thermal properties of these materials at their operating temperature (beyond 1000 °C) is crucial [1]. One of the main challenges lies in the development of direct models taking into account the strong conduction-radiation coupling in the sample at high temperature [2, 3]. The heat transfer by radiation in a participating medium (emitting/absorbing and scattering) needs to be considered as well as the potentially complex geometry of the experimental set-up and the sample. Moreover, in order to be used in an estimation methodology, this coupled model needs to offer a decent compromise between accuracy and speed of execution during model resolution.

So far, in most of the inverse processes associated to the thermal properties estimations (thermal conductivity or diffusivity, for instance), either purely conductive model are used or coupled models using assumptions on the optical properties (no scattering events, grey medium etc.) [4, 5]. Hence, a robust coupled direct model in which these assumptions may be lifted and without limitation to asymptotic approach (optically thick or

*Corresponding Author: lea.penazzi@univ-lorraine.fr

thin media) is needed. Previous studies demonstrated the feasibility and relevance of using the Monte Carlo method to solve coupled and transient thermal problems in the context of complex media characterization [6].

In the present work, the development and resolution of a coupled conduction-radiation model in a semi-transparent media is addressed. The studied configuration is a standard academic case corresponding to a two-dimensional square enclosure containing an absorbing/emitting and non-scattering grey medium bounded by black walls. Heat conduction is considered at transient state and is coupled to volumetric radiation. When Mishra et al. [7] investigated this transient problem, the heat transfer equation was solved using alternatively a Finite-Volume Method (FVM) and a Lattice Boltzmann Method (LBM), while the radiative source term was calculated using the the Collapsed-Dimension Method (CDM). This reference case was as well studied by Asllanaj et al. [8]. They used the FVM to solve the radiative source term based on a cell vertex scheme and associated to a modified exponential scheme. The heat transfer equation was solved using low or high order finite elements. Their results were in agreement with Mishra et al. [7] results.

In this study, the transient conduction is solved by Finite Differences Method (FDM) and the volumetric radiation is solved by the Monte Carlo Method (MCM). The originality and interest of this approach lies in the functional estimation of the radiative source term with the MCM allowing to evaluate the temperature field in a highly reduced computational time compared to conventional methods. This functional estimation is carried out without any compromise neither on the complexity of the coupled physics nor the geometry. The purpose of this study is to present a proof–of–concept of the method on an academic case that can be expanded to more complex cases in the future. First, the model of the academic configuration is presented, then, the algorithm of resolution is introduced including the functional estimation of the radiative source term with the MCM coupled with the FDM resolution. Finally, the results are presented, compared to the numerical solutions of Mishra et al. [7] used as a benchmark and conclusions are drawn.

2. THE FUNCTIONAL ESTIMATION MODEL

2.1 Studied configuration The studied configuration is illustrated on Fig. 1, which corresponds to a square enclosure of unit length (L =1 m) containing a non scattering gray medium ($k_s = 0$). The optical thickness $\tau = \beta L = (k_a + k_s)L$ is equal to 1, as the absorption coefficient k_a is equal to $1\mathrm{m}^{-1}$, and the medium boundaries are black surfaces ($\epsilon = 1$) with imposed temperatures. The reference temperature T_{hot} is the temperature of the bottom wall $\partial\mathcal{D}_{\mathrm{hot}}$. The other surface temperatures are cold and equal to $T_{\mathrm{cold}} = T_{\mathrm{hot}}/2$ (on the surface $\partial\mathcal{D}_{\mathrm{cold}}$). Heat conduction is at transient state and at initial time, the temperature of the medium is set equal to T_{cold}. The heat transfer model equations are the following :

$$\begin{cases} \rho C_{\mathrm{p}} \dfrac{\partial T}{\partial t} - \lambda \Delta T = -\vec{\nabla} \cdot \vec{q}_{\mathrm{R}} & \forall \vec{x} \in \mathcal{D}, \forall t > 0 \quad (1) \\ T(\vec{x}, 0) = T_{\mathrm{cold}} & \forall \vec{x} \in \mathcal{D}, t = 0 \quad (2) \\ T(\vec{x}, t) = T_{\mathrm{hot}} & \forall \vec{x} \equiv \vec{y}_{\mathrm{hot}} \in \partial\mathcal{D}_{\mathrm{hot}}, \forall t > 0 \quad (3) \\ T(\vec{x}, t) = T_{\mathrm{cold}} & \forall \vec{x} \equiv \vec{y}_{\mathrm{cold}} \in \partial\mathcal{D}_{\mathrm{cold}}, \forall t > 0 \quad (4) \end{cases}$$

The radiative source term from Eq. (1) may be obtained from a radiative balance of a homogeneous and isothermal volume $\mathcal{V}$ expressed as follows:

$$\boldsymbol{\Phi}_{\mathcal{V}} = \int_{\mathcal{V}} (\vec{\nabla} \cdot \vec{q}_{\mathrm{R}})\, d\mathcal{V} = \int_{\mathcal{V}} d\mathcal{V} \int_{4\pi} d\vec{\omega}\, k_{\mathrm{a}} \left(\boldsymbol{\mathcal{I}}^{\mathrm{eq}}(\vec{x}) - \boldsymbol{\mathcal{I}}(\vec{x}, \vec{\omega}) \right) \quad (5)$$

The medium being grey, the optical properties and the radiative intensity do not depend on frequency. In this equation, $d\vec{x}$ corresponds to an elementary volume element and $d\vec{\omega}$, to the solid angle. The black body

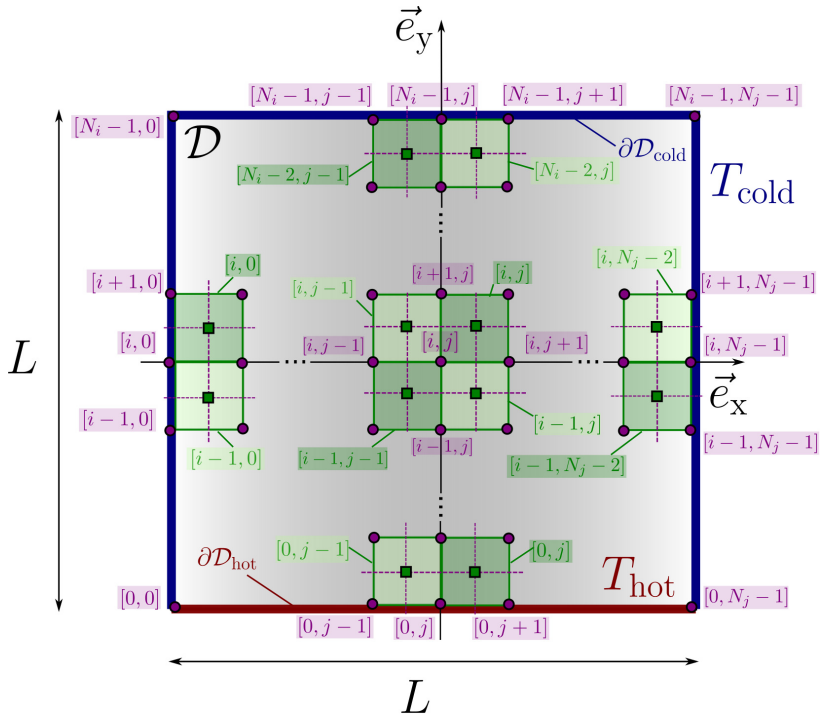

Fig. 1 Schematic view of the 2D configuration defining the academic thermal problem from [7, 8]. Conductive nodes are represented with purple circles and radiative nodes, with green squares.

intensity $\mathcal{I}^{\mathrm{eq}}$ at the location $\vec{x}$ is expressed as:

$$\mathcal{I}^{\mathrm{eq}}(\vec{x}) = \frac{\sigma_{\mathrm{SB}}}{\pi} T^4(\vec{x}) \tag{6}$$

With σ_{SB}, the Stefan–Boltzmann constant and $T(\vec{x})$ the temperature at the $\vec{x}$ location. $\mathcal{I}(\vec{x},\vec{\omega})$ is the radiative intensity at the location $\vec{x}$ in the direction $\vec{\omega}$ and is solution of the following Radiative Transfer Equation (RTE):

$$\begin{aligned}\vec{\omega}.\vec{\nabla}\mathcal{I}(\vec{x},\vec{\omega}) = &-(k_{\mathrm{a}}+k_{\mathrm{s}})\mathcal{I}(\vec{x},\vec{\omega}) + k_{\mathrm{a}}\mathcal{I}^{\mathrm{eq}} \\ &+ k_{\mathrm{s}}\int_{4\pi} \mathrm{P}(\vec{x},\vec{\omega}|\vec{\omega}')\mathcal{I}(\vec{x},\vec{\omega}')d\vec{\omega}'\end{aligned} \tag{7}$$

Where $\vec{\omega}$ is the unit direction, k_{s}, the scattering coefficient and P, the scattering phase function. The refractive index n_{r} is equal to 1.

2.2 Heat conduction numerical resolution The temporal term $\frac{\partial T}{\partial t}$, is discretized with a explicit first-order Euler method and the laplacian term ΔT is approximated with a second-order difference approximation. The heat equation corresponding to Eq. (1) becomes :

$$\frac{T^{\mathrm{n}}_{\mathrm{i,j}} - T^{\mathrm{n-1}}_{\mathrm{i,j}}}{\delta_{\mathrm{t}}} - \alpha\left(\frac{T^{\mathrm{n-1}}_{\mathrm{i-1,j}} + T^{\mathrm{n-1}}_{\mathrm{i+1,j}} - 4T^{\mathrm{n-1}}_{\mathrm{i,j}} + T^{\mathrm{n-1}}_{\mathrm{i,j-1}} + T^{\mathrm{n-1}}_{\mathrm{i,j+1}}}{\delta^2_{\mathrm{x}}}\right) = -\frac{1}{\rho C_{\mathrm{p}}} S^{\mathrm{n-1}}_{\mathrm{ray,i,j}} \tag{8}$$

With the spatial step δ_{x} (identical for both dimensions, i.e. $\delta_{\mathrm{x}} = \delta_{\mathrm{y}}$), the time step, δ_{t} and the thermal diffusivity, $\alpha = \frac{\lambda}{\rho C_{\mathrm{p}}}$. As represented in Fig. 1, the 2D medium is discretized into a number $N_i \times N_j$ of

conductive meshes. The conduction mesh is cartesian regular with $N_i = N_j$. The conduction meshes are indexed with i ranging from 0 to $N_i - 1$ and j ranging from 0 to $N_j - 1$. Each node $[i, j]$ (represented using purple circles on Fig. 1) is located at the center of a conductive mesh and each mesh has a surface equal to δ_{x}^2. In the finite differences method, the assumption made is that the temperature of each conductive mesh is homogeneous. Reformulating Eq. (8), leads to the following expression for the temperature at a position (x, y) and time t :

$$T_{\mathrm{i,j}}^{\mathrm{n}} = \left(1 - 4\frac{\alpha\delta_{\mathrm{t}}}{\delta_{\mathrm{x}}^2}\right) T_{\mathrm{i,j}}^{\mathrm{n-1}} + \frac{\alpha\delta_{\mathrm{t}}}{\delta_{\mathrm{x}}^2}\left(T_{\mathrm{i-1,j}}^{\mathrm{n-1}} + T_{\mathrm{i+1,j}}^{\mathrm{n-1}} + T_{\mathrm{i,j-1}}^{\mathrm{n-1}} + T_{\mathrm{i,j+1}}^{\mathrm{n-1}}\right) - \frac{\delta_{\mathrm{t}}}{\rho C_{\mathrm{p}}} S_{\mathrm{ray,i,j}}^{\mathrm{n-1}} \tag{9}$$

In this case, the Courand-Friedrichs-Lewis (CFL) condition states that $\mu \leq 1/4$ so that this explicit scheme remains stable. The previous Eq. (9) remains valid for $i \in \{\ 1\ :\ N_i - 2\}$ and $j \in \{\ 1\ :\ N_j - 2\}$. For the boundary nodes located either on the cold surfaces (when $\vec{y}_{\mathrm{cold}} \in \partial\mathcal{D}_{\mathrm{cold}}$, see Fig. 1) on the hot surface (when $\vec{y}_{\mathrm{hot}} \in \partial\mathcal{D}_{\mathrm{hot}}$, see Fig. 1), the temperature values are set respectively to T_{cold} and T_{hot}.

The volumetric source term S_{ray} (in $\mathrm{W\,m^{-3}}$) is computed at each iteration of the finite differences algorithm for each conductive node $[i, j]$. To this end, the radiative source term $\boldsymbol{\Phi}_{\mathcal{S}}$[1] is estimated for each radiative node and then equally allocated between the four conductive nodes nearby, such as :

$$S_{\mathrm{ray,i,j}}^{\mathrm{n-1}} = \frac{\boldsymbol{\Phi}_{\mathcal{S},\mathrm{i-1,j-1}}^{\mathrm{n-1}} + \boldsymbol{\Phi}_{\mathcal{S},\mathrm{i-1,j}}^{\mathrm{n-1}} + \boldsymbol{\Phi}_{\mathcal{S},\mathrm{i,j}}^{\mathrm{n-1}} + \boldsymbol{\Phi}_{\mathcal{S},\mathrm{i,j-1}}^{\mathrm{n-1}}}{4\delta_{\mathrm{x}}^2} \tag{10}$$

The radiative mesh is chosen slightly shifted from the conductive mesh and in each radiative mesh, the radiative source term $\boldsymbol{\Phi}_{\mathcal{S}}$ is homogeneous. In Fig. 1, the $(N_i - 1) \times (N_j - 1)$ radiative meshes (represented in green squares) are indexed with i from 0 to $N_i - 2$ and j from 0 to $N_j - 2$.

2.3 Estimation of the radiative source term with the MCM For each of the $(N_i - 1)(N_j - 1)$ radiative node, a Monte Carlo computation is required to estimate the radiative source term $\boldsymbol{\Phi}_{\mathcal{S}}$. The expression of the source term in Eq. (5) needs to be translated in statistical terms to estimate it with a Monte Carlo algorithm. Given the expression of the solid angle $d\vec{\omega} = d\varphi\ \sin\theta d\theta$ depending on the polar and azimuthal angles denoted respectively θ and φ, the radiative source term may be expressed as :

$$\boldsymbol{\Phi}_{\mathcal{S}} = \int_{D} p_{\mathrm{X}}(\vec{x})\, d\vec{x} \int_{2\pi} p_{\boldsymbol{\Phi}}(\varphi)\, d\varphi \int_{0}^{\pi} p_{\Theta}(\theta)\, d\theta\ \underbrace{4\pi\ \delta_{\mathrm{x}}^2\ k_{\mathrm{a}}\left(\mathcal{I}^{\mathrm{eq}} - \mathcal{I}(\vec{x}, \vec{\omega})\right)}_{\text{Monte Carlo weight } w_{\mathrm{k}}} \tag{11}$$

The previous equation can be given a statistical interpretation by introducing the probability density functions. The probability density $p_{\mathrm{X}}(\vec{x}) = \frac{1}{S} = \frac{1}{\delta_{\mathrm{x}}^2}$ corresponds to the sampling of a starting position in the 2D radiative mesh and $p_{\Theta}(\theta) = \frac{\sin\theta}{2}$ and $p_{\boldsymbol{\Phi}}(\varphi) = \frac{1}{2\pi}$ are the probability density corresponding respectively to the sampling of the polar and azimutal angles necessary to the unit direction $\vec{\omega}$ sampling. The previous Eq. (11) may be interpreted as the expectation of a random variable W, the Monte Carlo weight, such as $\boldsymbol{\Phi}_{\mathcal{S}} = \mathbb{E}(W)$. A Monte Carlo computation consists in sampling N_{MC} optical paths, providing N_{MC} realizations $w_1, w_2 ... w_{N_{\mathrm{MC}}}$ of W, and estimate the radiative source term $\boldsymbol{\Phi}_{\mathcal{S}}$ as the mean value m of these Monte Carlo weights realizations, such as $\boldsymbol{\Phi}_{\mathcal{S}} \approx m = \frac{1}{N_{\mathrm{MC}}} \sum_{k=1}^{N_{\mathrm{MC}}} w_{\mathrm{k}}$ as well as the associated uncertainty $s = \frac{1}{\sqrt{N_{\mathrm{MC}}}} \left(\frac{1}{N_{\mathrm{MC}}} \sum_{k=1}^{N_{\mathrm{MC}}} w_{\mathrm{k}}^2 - m^2\right)^{\frac{1}{2}}$. The essence of the path sampling, represented on the Fig. 2 is as follows.

[1]The heat flux $\boldsymbol{\Phi}_{\mathcal{V}}$ in W estimated in Eq. (5) becomes surfacic and expressed as follows $\boldsymbol{\Phi}_{\mathcal{S}} = \int_{\mathcal{S}} (\vec{\nabla} \cdot \vec{q}_{\mathrm{R}})\ d\mathcal{S} = \int_{\mathcal{S}} d\mathcal{S} \int_{4\pi} d\vec{\omega}\ k_{\mathrm{a}} \left(\mathcal{I}^{\mathrm{eq}}(\vec{x}) - \mathcal{I}(\vec{x}, \vec{\omega})\right)$ in $\mathrm{W\,m^{-1}}$.

A start position $\vec{x}_{\text{start}}$ is sampled uniformly within the medium $\mathcal{D}$ according to $p_{\text{X}}(\vec{x})$. The current position $\vec{x}_{\text{c}}$ value is initialized at the value $\vec{x}_{\text{start}}$. Then, a direction $\vec{\omega}$ is sampled with the successive sampling of the angles φ and θ according to the probabilities densities $p_{\Phi}(\varphi)$ and $p_{\Theta}(\theta)$. An extinction length l is sampled according to the exponential Beer-Lambert law (depending on the extinction coefficient $\beta = k_{\text{a}} + k_{\text{s}}$) and the current position $\vec{x}_{\text{c}}$ value is actualized to $\vec{x}_{\text{c}} + l\vec{\omega}$. A test is performed to identify if the current location $\vec{x}_{\text{c}}$ is stil in the volume $\mathcal{D}$ or at one of the medium boundary, either $\partial\mathcal{D}_{\text{cold}}$ or $\partial\mathcal{D}_{\text{hot}}$. If $\vec{x}_{\text{c}} \in \mathcal{D}$, an absorption event occurs and the path stops at the location $\vec{x}_{\text{c}}$ (see (1) in Figs. 2 et 3). The path's end location $\vec{x}_{\text{end}}$ is set equal to $\vec{x}_{\text{c}}$ and the Monte Carlo weight is stored. If $\vec{x}_{\text{c}}$ is not in the volume $\mathcal{D}$, a test is performed to know at which boundary is the current location. An absorption event occurs either at the $\partial\mathcal{D}_{\text{hot}}$ boundary and the path stops at the location $\vec{x}_{\text{c}} \equiv \vec{y}_{\text{hot}}$ (see (2) in Figs. 2 et 3) or at the $\partial\mathcal{D}_{\text{cold}}$ boundary and the path stops at the location $\vec{x}_{\text{c}} \equiv \vec{y}_{\text{cold}}$ (see (3) in Figs. 2 et 3), then the corresponding Monte Carlo weight is stored. As indicated in Eq. (11), the Monte Carlo weight w_{k} stored at the end of each path contains the difference between the emitted radiant intensity $\mathcal{I}^{\text{eq}}$ and the absorbed radiant intensity $\mathcal{I}(\vec{x}, \vec{\omega})$ for a given location $\vec{x}$ and direction $\vec{\omega}$. Translated in algorithmic terms, w_{k} contains the difference between the black body intensity emitted in a mesh $[\text{i}_{\text{start}}, \text{j}_{\text{start}}]$ and the black body intensity absorbed in a mesh $[\text{i}_{\text{end}}, \text{j}_{\text{end}}]$, i.e. $w_{\text{k}} = 4\pi\delta_{\text{x}}^2 k_{\text{a}} \left(\mathcal{I}^{\text{eq}}[\text{i}_{\text{start}}, \text{j}_{\text{start}}] - \mathcal{I}^{\text{eq}}[\text{i}_{\text{end}}, \text{j}_{\text{end}}]\right)$.

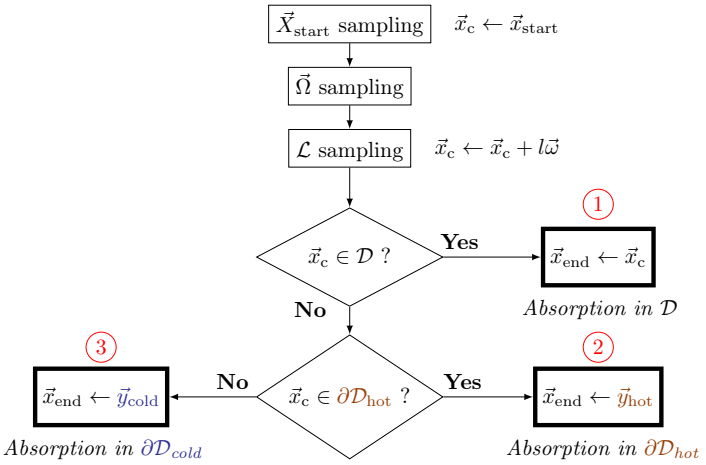

Fig. 2 Path sampling algorithm corresponding to a k^{th} realization of the Monte Carlo algorithm to estimate $\Phi_{\mathcal{S}}$.

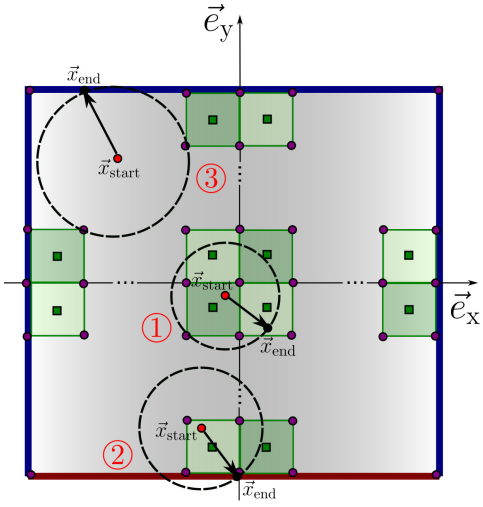

Fig. 3 Examples of random paths inside the square enclosure according to the algorithm from Fig. 2.

2.4 The corresponding functional estimation of the radiative source term The radiative source term $\Phi_{\mathcal{S}}$ needs to be evaluated for each of the $(N_i - 1)(N_j - 1)$ radiative mesh at each iteration on the Finite Differences (FD) algorithm. At each calculation of the source term, N_{MC} optical paths are sampled. These operations may be time consuming and can be questioned when one notices that at each iteration of the FD algorithm, only one set of values change in input of the MC algorithm : the list of temperature at each node to the power 4. Given the fact that each time the $(N_i - 1)(N_j - 1)$ radiative source terms $\Phi_{\mathcal{S}}[\text{i,j}] \equiv \Phi_{\mathcal{S}}[\text{i}_{\text{start}}, \text{j}_{\text{start}}]$ the only values changing in input are the equilibrium radiative intensities $\mathcal{I}^{\text{eq}}$ computed, i.e. the list of temperatures $T[\text{i,j}]^4 \equiv T[\text{i}_{\text{end}}, \text{j}_{\text{end}}]^4$. This can be noticed by injecting Eq. (6) in Eq. (11) and express the estimated radiative source term at the $[\text{i}_{\text{start}}, \text{j}_{\text{start}}]$ as follows :

$$\boldsymbol{\Phi}_{\mathcal{S}}[\mathrm{i_{start}},\mathrm{j_{start}}] \approx \frac{1}{N_{\mathrm{MC}}}\sum_{k=1}^{N_{\mathrm{MC}}} 4\sigma_{\mathrm{SB}}\delta_{\mathrm{x}}^2 k_{\mathrm{a}}\left(T[\mathrm{i_{start}},\mathrm{j_{start}}]^4 - T[i_{\mathrm{end},k},j_{\mathrm{end},k}]^4\right)$$

$$\Leftrightarrow \boldsymbol{\Phi}_{\mathcal{S}}[\mathrm{i_{start}},\mathrm{j_{start}}] \approx 4\sigma_{\mathrm{SB}}\delta_{\mathrm{x}}^2 k_{\mathrm{a}}(T[\mathrm{i_{start}},\mathrm{j_{start}}]^4 - \underbrace{\frac{1}{N_{\mathrm{MC}}}\sum_{k=1}^{N_{\mathrm{MC}}} T[i_{\mathrm{end},k},j_{\mathrm{end},k}]^4}_{\text{(A)}}) \tag{12}$$

The second part (A) of the previous equation can be reformulated as :

$$\text{(A)} = \frac{1}{N_{\mathrm{MC}}}\sum_{k=1}^{N_{\mathrm{MC}}}\left(\mathcal{H}(i_{\mathrm{end},k}=0;j_{\mathrm{end},k}=0)T[0,0]^4 + ... + \mathcal{H}(i_{\mathrm{end},k}=N_i-1;j_{\mathrm{end},k}=N_j-1)T[N_i-1,N_j-1]^4\right) \tag{13}$$

In which $\mathcal{H}$ is the Heaviside function equal to 1 if the condition is satisfied and 0 otherwise. For the first term, at the end of the k^{th} path, if $i_{\mathrm{end},k}=0$ and $j_{\mathrm{end},k}=0$, $\mathcal{H}$ is equal to 1.

$$\frac{1}{N_{\mathrm{MC}}}\sum_{k=1}^{N_{\mathrm{MC}}} T[i_{\mathrm{end},k},j_{\mathrm{end},k}]^4 = \frac{1}{N_{\mathrm{MC}}}\underbrace{\left(N_{0,0}T[0,0]^4 + ... + N_{N_i-1,N_j-1}T[N_i-1,N_j-1]^4\right)}_{\sum_{i=0}^{N_i-1}\sum_{j=0}^{N_j-1}\frac{N_{i,j}}{N_{\mathrm{MC}}}T[i,j]^4} \tag{14}$$

In this way, the latter expression can be transformed so that at the end of the MC calculation, counters stored the number of times a path ended in this or that mesh $[i,j]$. For instance, $N_{0,0}$ stores the number of path that ended in mesh indexed $[0,0]$ out of a total of N_{MC} paths.

Hence, replacing the latter expression in (A) from Eq. (12) leads to the following expression :

$$\boldsymbol{\Phi}_{\mathcal{S}}[\mathrm{i_{start}},\mathrm{j_{start}}] \approx 4\sigma_{\mathrm{SB}}\delta_{\mathrm{x}}^2 k_{\mathrm{a}}\left(T[\mathrm{i_{start}},\mathrm{j_{start}}]^4 - \sum_{i=0}^{N_i-1}\sum_{j=0}^{N_j-1}\frac{N_{i,j}}{N_{\mathrm{MC}}}T[i,j]^4\right) \tag{15}$$

In order to estimate the $\boldsymbol{\Phi}_{\mathcal{S}}[\mathrm{i_{start}},\mathrm{j_{start}}]$ as a function of the whole temperature field, a single Monte Carlo computation may be performed in which, instead of storing the Monte Carlo weight w_k as expressed previously, the only coefficients needed to be stored are each $N_{i,j}$ corresponding to the number of times the radiative paths have been absorbed in the mesh $[i,j]$ during the Monte Carlo calculation (including the mesh boundaries).

Concretely, before starting the finite differences algorithm, $(N_i-1)(N_j-1)$ Monte Carlo computations are perfomed only once to estimate each $\boldsymbol{\Phi}_{\mathcal{S}}[\mathrm{i,j}]$ as a function of the temperature list at each conductive node to the power 4, such as $\boldsymbol{\Phi}_{\mathcal{S}}[\mathrm{i,j}] = \mathrm{f}\left(\overline{\overline{(T_{\mathrm{i,j}}^{\mathrm{n}-1})^4}}\right)$. For each of the $(N_i-1)(N_j-1)$ radiative source terms $\boldsymbol{\Phi}_{\mathcal{S}}[\mathrm{i,j}]$, at each Monte Carlo computation, $N_i \times N_j$ coefficients $\frac{N_{i,j}}{N_{\mathrm{MC}}}$ are computed. These $\frac{N_{i,j}}{N_{\mathrm{MC}}}$ coefficients may be assimilated to volumetric view factor informing on how each radiative mesh element sees another. Similarly as previously, the associated uncertainty of each Monte Carlo computation may be estimated. In this way, the temperature field to the power 4 corresponding to the matrix $\overline{\overline{(T_{\mathrm{i,j}}^{\mathrm{n}-1})^4}}$ is injected in the function at each iteration of the FD algorithm to estimate the $\boldsymbol{\Phi}_{\mathcal{S}}[\mathrm{i,j}]$.

2.5 Finite differences and Monte Carlo algorithm The finite differences algorithm operates with two temperature vectors. The first one, $\vec{T}_{\text{new}}$ gathers all the $N_i \times N_j$ values of the temperatures at the current time step n at each node [i, j]. The second, one $\vec{T}_{\text{old}}$ gathers all the $N_i \times N_j$ values of the temperatures at the previous n − 1 iteration.

Algorithm 2.1: Computation of the temperature profile $\vec{T}_{\text{new}}$ with the FEMC/FD algorithm.

for $i = 0 : N_i - 2$ **do**
  for $j = 0 : N_j - 2$ **do**
    Monte Carlo estimation of each of the $\frac{N_{i,j}}{N_{\text{MC}}}$ coefficients
  end
end
while $t < t_{max}$ **do**
  $\vec{T}_{\text{old}} \leftarrow \vec{T}_{\text{new}}$ *%Initialization*
  for $i = 1 : N_i - 1$ **do**
    for $j = 1 : N_j - 1$ **do**
      Computation of each of the $\boldsymbol{\Phi}_S$[i,j] (see Eq. (15))
    end
  end
  for $i = 0 : N_{nodes} - 1$ **do**
    for $j = 0 : N_{nodes} - 1$ **do**
      Calculation of S_{ray}[i,j] (see Eq. (10))
      Calculation of each $\vec{T}_{\text{new}}$[i,j] (see Eq. (9))
    end
  end
  $t \leftarrow t + \delta_{\text{t}}$
end

As described in the Algorithm 2.1, first, for each of the $(N_i - 1)(N_j - 1)$ element of the radiative mesh, all of the $(N_i - 1)(N_j - 1)$ $\frac{N_{i,j}}{N_{\text{MC}}}$ coefficients are estimated with the MC algorithm. This way, the radiative source term may be estimated afterwards as a function of the temperature field to the power 4. This method will be referred hereafter as the Function Estimation Monte Carlo (FEMC) method. Then in the FD algorithm, the $\vec{T}_{\text{old}}$ vector is firstly initialized with its values set equal to $\vec{T}_{\text{new}}$, corresponding now to the $(\text{n} - 1)^{\text{nth}}$ iteration (i.e. $T_{\text{i,j}}^{\text{n}-1}$). Then, for each radiative mesh element [i,j], each source term $\boldsymbol{\Phi}_S$[i,j], is estimated thanks to the functional relation presented previously and the coefficients estimated with the FEMC method. Afterward, for each conductive node [i,j] the radiative source term S_{ray}[i,j] is computed. Eventually, the corresponding $\vec{T}_{\text{new}}$[i,j] profile at the $(\text{n})^{\text{nth}}$ time step of the finite differences algorithm can be computed (i.e. $T_{\text{i,j}}^{\text{n}}$). The algorithm proceeds to the next time step by adding δ_{t} to the current time t until the maximum time t_{max} is reached. If t_{max} corresponds to the steady state time a tolerance criterion is set, the ratio $\frac{|\vec{T}_{\text{new}}[\text{i,j}] - \vec{T}_{\text{old}}[\text{i,j}]|}{\vec{T}_{\text{old}}[\text{i,j}]}$ should be lower than 1×10^{-5}.

3. RESULTS

The pure grey absorbing medium $\mathcal{D}$ with black walls presented in Section 2.1 is studied (see Fig. 1). The medium is initially at a temperature T_{cold} =50 K. At a time $t > 0$, the temperature on the bottom wall ($y = 0$) rises from T_{cold} =50 K to T_{hot} =100 K within one dimensionless time step and then remains constant

Table 1 Computation times (in seconds) for the pure absorbing case with black walls.

	Stark number $\mathcal{N}$ (-)		
Dimensionless time ξ (-)	0.01	0.1	1
0.001		1.7	
0.005		8.2	
0.015		24.4	
0.04		65.9	
0.06	99.7		
0.17		284	
0.2			340

[1] The CPU time to obtain the functional Monte Carlo coefficients is 4 h on an Intel®Xeon™E5 2.10 GHz

[2] Computing times are given for an Intel®Core™i5-10210U CPU 1.60GHz

indefinitely. The T_{hot} temperature is considered as the reference temperature. The other faces of the square enclosure are kept constant at T_{cold} during this time.

To quantify the relative contribution of conduction versus radiation, a dimensionless parameter is introduced, the Stark number (also named as the conduction–radiation parameter) expressed as $\mathcal{N} = \frac{\lambda k_{\text{a}}}{4\sigma_{\text{SB}} T_{\text{hot}}^3}$. Given the value of T_{hot} =100 K, as well as k_{a} =1 m^{-1}, if the value of the Stark number $\mathcal{N}$ is set, the thermal conductivity value λ may be calculated with the following expression $\lambda = \frac{\mathcal{N} 4\sigma_{\text{SB}} T_{\text{hot}}^3}{k_{\text{a}}}$. For large values of $\mathcal{N}$, conduction predominates over radiation and, on the opposite, for small values of $\mathcal{N}$, radiation predominates. Three cases are presented in which $\mathcal{N}$ is set equal to 0.01, 0.1 and 1. In order to compare these cases a dimensionless time parameter is introduced : $\xi = \alpha k_{\text{a}}^2 t$. The results are compared at different instants $\xi = \{\ 0.001, 0.005, 0.015, 0.04\}$ and three differents values corresponding for each to the steady state, $\xi = 0.06, 0.17, 0.2$ for respectively $\mathcal{N} = 0.01, 0.1, 1$. For these given values of the Stark numbers and dimensionless time parameters, the temperature profiles on the centerline ($x = L/2$ and $y \in [0, L]$) are computed with the FEMC/FD algorithm and presented on Fig. 4 . Each of these temperature profiles (denoted with red-filled bullets) are compared to results from two different numerical methods from Mishra et al. [7], i.e. the FVM method (represented with grey-filled triangles) and the LBM method (represented with blue continuous lines). The results from the FEMC/MC method are in good agreement with results from the reference case.

As presented in Tab. 1, one of the major benefit of the FEMC/FD algorithm is to enable a significant computational time reduction compared to the original MC/FD algorithm. Indeed, to produce this whole set of results for differents values of Stark number and dimensionless time step, only a single FEMC computation was necessary to estimate the function's coefficient and the calculation lasted 4 h (see Tab. 1) for $N_{\text{MC}} = 10\,000\,000$ and a total of 21×21 conductive nodes. After this, each of the 15 graphs (3 values of $\mathcal{N}$, for each 5 values of ξ) were computed with the FD algorithm in less than approximately 1min for transient state and a maximum value of 340s at steady state (see $\xi = 0.2$ and $\mathcal{N} = 1$ on Tab. 1).

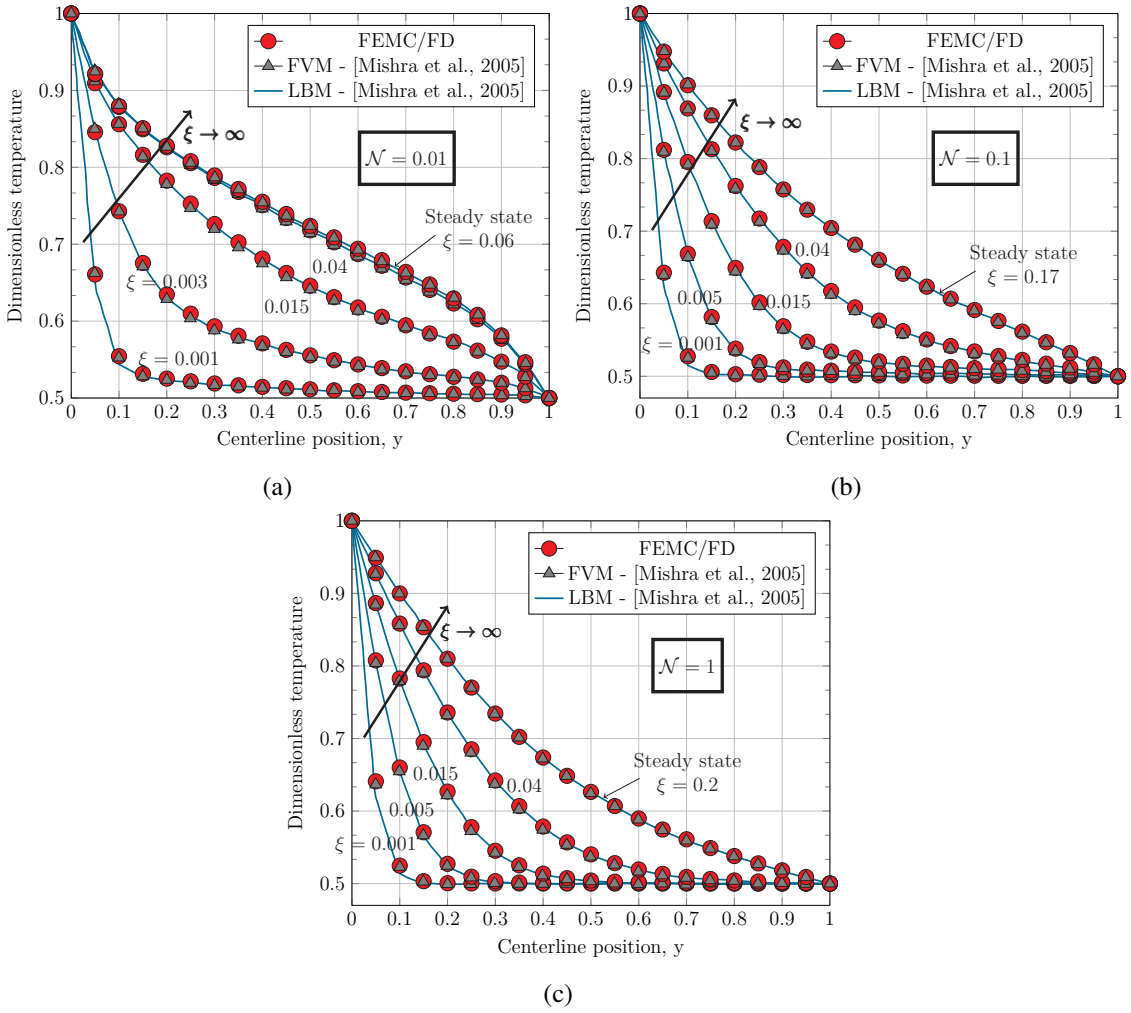

Fig. 4 Dimensionless temperature distribution along the centerline position at different dimensionless times and for three different values of the Stark number $\mathcal{N}$.

4. CONCLUSIONS

The present study was a proof of concept in which the radiative source term of the heat equation was evaluated as a function of the temperature field to the power 4 without linearization of the radiative heat transfer. This feature proved to be interesting in order to reduce the computation time required for the resolution of the coupled conduction-radiation heat transfer in a semi-transparent medium at transient state. Indeed, this function was obtained without any assumption on the radiative behaviour of the physics and is not limited to grey media, the dependency of the radiative properties on the frequency may be taken into account. The scattering character of the medium will be studied in further configurations and does not pose any particular difficulties as these may be compared to literature results from [7]. Furthermore, the development of this method is not limited to academic configuration and may be extended to more complex geometries (2D/3D). For all of these reasons, to consider the development and implementation of the FEMC/FD method in inversion processes becomes practicable as the direct model needs to be 1) as realistic as possible and 2) a compromise between precision and being solved within a reasonable time. Further developments may be continued to implement this direct coupled model in a practical configuration in order to carry out a sensitivity study to the various influencing parameters before the inverse process. The method will be developed specifically for use in inversing parallel hot wire measurements [2].

ACKNOWLEDGMENT

High Performance Computing resources were partially provided by the EXPLOR centre hosted by the University of Lorraine (Project: 2020EMPPX2210).

REFERENCES

[1] Machin, G., Anhalt, K., Battuello, M., Bourson, F., Dekker, P., Diril, A., Edler, F., Elliott, C., Girard, F., Greenen, A., Kňazovická, L., Lowe, D., Pavlásek, P., Pearce, J., Sadli, M., Strnad, R., Seifert, M. and Vuelban, E., "The European project on high temperature measurement solutions in industry (HiTeMS) – A summary of achievements", *Measurement*, 78, pp. 168–179, doi:https://doi.org/10.1016/j.measurement.2015.09.033, Available at https://www.sciencedirect.com/science/article/pii/S026322411500500X (2016).

[2] Penazzi, L., Jannot, Y., Meulemans, J., Farges, O. and Schick, V., "Influence of radiation heat transfer on parallel hot-wire thermal conductivity measurements of semi-transparent materials at high temperature", *International Journal of Thermal Sciences*, 179, p. 107690, doi:https://doi.org/10.1016/j.ijthermalsci.2022.107690, Available at https://www.sciencedirect.com/science/article/pii/S1290072922002253 (2022).

[3] Zhang, H., Ma, Y., Wang, X. and Tang, G., "Numerical study of the influence of thermal radiation on measuring semi-transparent thermal insulation material with hot wire method", *International Communications in Heat and Mass Transfer*, 121, p. 105120, doi:https://doi.org/10.1016/j.icheatmasstransfer.2021.105120, Available at https://www.sciencedirect.com/science/article/pii/S0735193321000142 (2021).

[4] Jannot, Y. and Degiovanni, A., "An improved model for the parallel hot wire: Application to thermal conductivity measurement of low density insulating materials at high temperature", *International Journal of Thermal Sciences*, 142, pp. 379–391, doi:https://doi.org/10.1016/j.ijthermalsci.2019.04.026, Available at https://www.sciencedirect.com/science/article/pii/S1290072918320088 (2019).

[5] Jannot, Y., Degiovanni, A., Schick, V. and Meulemans, J., "Thermal diffusivity measurement of insulating materials at high temperature with a four-layer (4L) method", *International Journal of Thermal Sciences*, 150, p. 106230, doi:https://doi.org/10.1016/j.ijthermalsci.2019.106230, Available at https://www.sciencedirect.com/science/article/pii/S1290072919312529 (2020).

[6] Sans, M., Schick, V., Parent, G. and Farges, O., "Experimental characterization of the coupled conductive and radiative heat transfer in ceramic foams with a flash method at high temperature", *International Journal of Heat and Mass Transfer*, 148, p. 119077, doi:https://doi.org/10.1016/j.ijheatmasstransfer.2019.119077, Available at https://www.sciencedirect.com/science/article/pii/S0017931019311846 (2020).

[7] Mishra, S. C., Lankadasu, A. and Beronov, K. N., "Application of the lattice Boltzmann method for solving the energy equation of a 2-D transient conduction–radiation problem", *International Journal of Heat and Mass Transfer*, 48(17), pp. 3648–3659, doi:https://doi.org/10.1016/j.ijheatmasstransfer.2004.10.041, Available at https://www.sciencedirect.com/science/article/pii/S0017931005000864 (2005).

[8] Asllanaj, F., Parent, G. and Jeandel, G., "Transient Radiation and Conduction Heat Transfer in a Gray Absorbing-Emitting Medium Applied on Two-Dimensional Complex-Shaped Domains", *Numerical Heat Transfer, Part B: Fundamentals*, 52(2), pp. 179–200, doi:10.1080/10407790701227351, Available at https://doi.org/10.1080/10407790701227351 (2007).